*Skin Research and Technology 2005; **11**: 236–241*
Printed in Denmark · All rights reserved

Skin Research and Technology

Pigment distribution in melanocytic lesion images: a digital parameter to be employed for computer-aided diagnosis

S. Seidenari[1], G.Pellacani[1] and C. Grana[2]

[1]*Department of Dermatology and* [2]*Department of Computer Engineering, University of Modena and Reggio Emilia, Modena, Italy*

Background/purpose: Since in early melanoma (MM) and especially in *in situ* MM differential structures, which are diagnostic for MM may be lacking, pigment distribution asymmetry represents an important diagnostic feature. Our aim was to automatically assess pigment distribution in images referring to MMs, atypical nevi (AN) and clearly benign nevi (BN), and to evaluate the diagnostic capability of numerical parameters describing a non homogeneous distribution of pigmentation.

Methods: An image analysis program enabling the numerical assessment of pigment distribution in melanocytic lesions (ML), based on evaluation and comparison of red, green, blue (RGB) colour components inside image colour blocks, was employed on 459 videomicroscopic digital images, referring to 95 MMs, 76 AN and 288 BN.

Results: Significant differences in pigment distribution parameters (mean RGB distance, variance and maximum distance) between the three ML populations were observed, permitting a good discrimination of MMs. On the test set comprising 230 lesion images, the area under the curve value of the receiver operating characteristic curve was 0.933. For a *D* score equal to 0, corresponding to the best diagnostic accuracy (86.6%), a sensitivity of 87.5% and a specificity of 85.7% were obtained.

Conclusion: This original evaluation method for digital pigment distribution, based on mathematical description and comparison of colours in different image blocks, provides numerical parameters to be implemented in image analysis programs for computer-aided MM diagnosis.

Key words: dermoscopy – epiluminescence microscopy – image analysis – melanoma – polarized light – videomicroscopy

Accepted for publication 13 November 2004

Increase in incidence and mortality rates for melanoma (MM) is observed worldwide. Early diagnosis with surgical removal of thin lesions is the only curative treatment. Dermoscopy, which employs incident light magnification systems associated to the epiluminescence technique or polarized light, has been introduced as an aid to clinical diagnosis (1–4). It is now widely established that this technique improves diagnostic accuracy for MM, especially for difficult-to-diagnose lesions (1–3). However, clinical as well as dermoscopic diagnosis of MMs is particularly difficult for *in situ*- or thin lesions, for which early identification could be particularly useful. Moreover, variability in the interpretation of dermoscopic images and poor reproducibility in pattern analysis is unavoidable and may lead to misdiagnoses (5). Instruments, providing the quantitative characterization of parameters of clinically significant features of melanocytic lesion (ML) images associated to statistical classification methods may represent the basis for computer-assisted differentiation between malignant and benign lesions (6–18). When employed by expert dermatologists, these may provide a support to dermoscopic diagnosis possibly leading to further improvement in diagnostic accuracy for MM.

The distribution of dermoscopic structures and colours represents an important element for dermoscopic diagnosis (19–22). Asymmetry of these structures contributes to the semiquantitative scoring system of Stolz et al. (4, 23). Also according to Blum et al. (24) structure asymmetry inside the lesion in at least one axis is scored together with shape asymmetry to reach a final result enabling the distinction between malignant and benign lesions. Since in early MM and especially

The authors have no conflict of interest to disclose.

in *in situ* MM differential structures which are diagnostic for MM may be lacking, network atypia and pigment distribution asymmetry represent important diagnostic features.

The aim of this study was to automatically assess pigment distribution in images referring to MMs, atypical nevi (AN) and clearly benign nevi (BN), and to evaluate the diagnostic capability of numerical parameters describing asymmetric distribution of pigmentation.

Materials and Methods

Image data base

Four hundred and fifty-nine ML images, referring to 76 AN, 288 BN and 95 MMs were studied. The images were subdivided into the three above subgroups according to clinical, dermoscopic and histopathologic evaluation. Histopathology was performed on AN and MMs, whereas only 30% of BN were excised and examined.

Image acquisition system

Images were acquired by means of a digital videomicroscope (VMS-110A, Scalar Mitsubishi, Tama-shi, Tokyo, Japan), with a 20-fold magnification enabling the whole lesion to be included in the monitor area. The instrument has been described elsewhere (10, 12). The images were digitized by means of a Matrox Orion frameboard and stored by an image acquisition program (VideoCap 8.09, DS-Medica, Milan, Italy), which runs under Microsoft Windows. The digitized images offer a spatial resolution of 768 $\times$ 576 pixels and a resolution of 16 million colours. The camera system is calibrated monthly on a set of colour patches with known colour properties (Gretag Machbet® ColorChecker Chart: Gretag Machbet, New Windsor, NY, USA) and the resulting colour profile is adjusted on the white test patch, between each patient's examination, according to a well defined procedure (25).

Image analysis program for pigment distribution assessment

After detection of the lesion border (16) and extraction of reference geometrical measures, such as centroid and main inertia axes, according to standard algorithms, pigment distribution asymmetry was assessed employing a three-step process for measuring the colour distribution inside the lesion. The first step consists in the elimination of colour details in the image and in its simplification into colour blocks. This is achieved by subdividing the image with a grid, after selecting the level of detail we are interested in (Fig. 1). The second step consists in colour description by computing the average colour inside each colour block, considering only pixels belonging to the lesion (Figs 1c, g). Image blocks are considered valid only if more than 25% of their area is constituted by lesion points, whereas they are excluded if less than 25% is comprised inside the lesion border (excluded blocks are shown in white in Figs 1d and h). The third algorithm phase assesses the colour difference

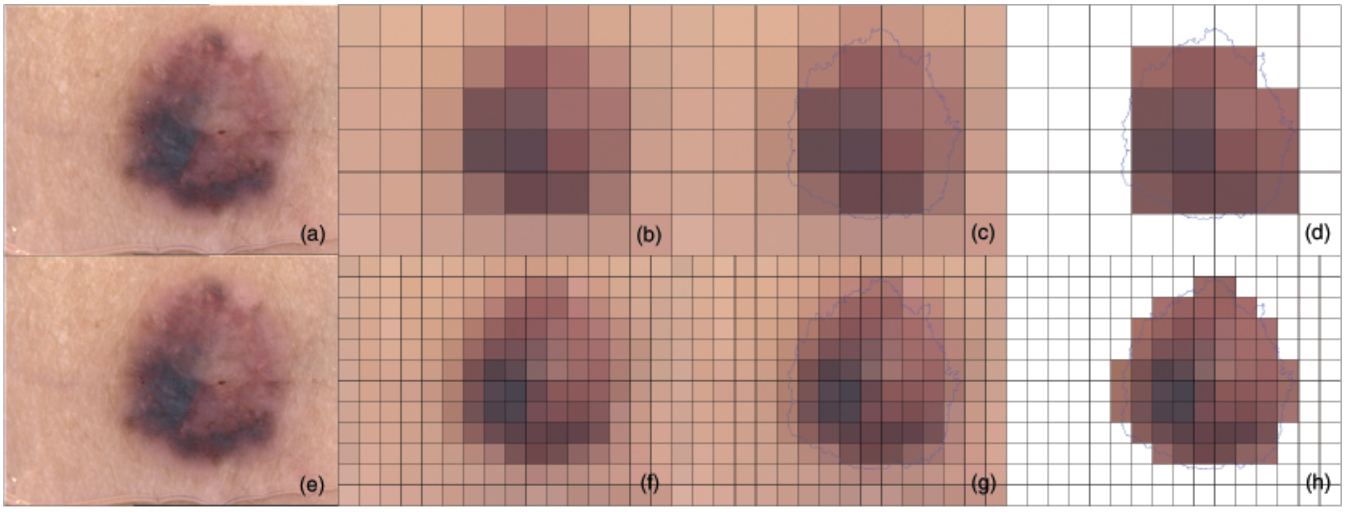

Fig. 1. Image analysis process for the assessment of structural asymmetry in melanocytic lesions images. The digital image (a) is subdivided by a grid (b, f). The average colour inside each colour block is computed, considering only pixels belonging to the lesion (c, g). Excluded blocks (when less than 25% is comprised inside the lesion border) are shown in white in d and h.

between blocks using the Euclidean distance in the red, green, blue (RGB) colour space, and extracts measures of colour distribution within the lesion image employing mean (PIXMED), variance (PIXVAR), and maximum colour differences (PIXMAX). This procedure was employed both on images composed by 91×96 pixels per block and on images composed by 48×49 pixels per block, equivalent to a resizing of the image to 1% and 2%, and corresponding to a mean number of valid blocks per image of 9.45 and 31.63, respectively. This process can produce a very high number of comparisons between pixels, since it needs $n(n-1)/2$ comparisons, where n is the number of valid pixels in the grid; this implies that up to 595 and 8385 distances, respectively, were computed for large lesions. Thus, we obtained a set of three parameters for each detail level (1% and 2%), corresponding to 6 measurements per lesion.

Statistics

For statistical analysis, the SPSS statistical package (release 10.0.06, 1999; SPSS Inc., Chicago, IL, USA) was used. As basic statistics, mean and standard deviation of computer values, i.e. mean, variance, and maximum colour differences, were calculated for MMs, AN, BN. Differences between values referring to the three lesion groups were evaluated using the Mann-Whitney *U*-test for independent samples. A *P*-values <0.01 was considered significant.

To examine the discriminant power of our numerical parameters for differentiating between nevi and MMs, discriminant analysis was performed on a training set comprising 50% of BN, AN and MMs (229 lesions). Discriminant analysis enables the identification of variables, which are important for distinction among the groups and develops a procedure for group classification based on a score attribution. A linear combination of independent variables is formed and serves as a basis for assigning cases to groups. A score (*D*), obtained for each lesion by the linear discriminant equation, is employed for the attribution of cases to groups. A receiver operating characteristic (ROC) analysis was performed to investigate sensitivity and specificity of the discriminant equation on classification of ML belonging to the test set, comprising the remaining 230 lesions. Diagnostic accuracy was estimated by the ratio between the percentage of the sum of true positives and true negatives, and the total number of lesions, and was calculated for each threshold (*D*) value. The area under the curve (AUC) and its 95% confidence interval (CI95%) were employed to estimate the probability of correctly classifying the lesions into benign and malignant.

Results

Mean and standard deviation of mathematical parameters calculated for BN, AN, and MMs are listed in Table 1. Mean distance, variance and maximum distance were significantly higher in MMs both in respect of BN and AN.

Among numerical parameters calculated by the computer, PIXMAX1, PIXMED2, PIXVAR2 and PIXMAX2 were selected by discriminant analysis for distinguishing between nevi and MMs of the training set. On the test set, the AUC value of the ROC curve was 0.933. For a *D* score equal to 0, corresponding to the best

TABLE 1. Computer parameters in clearly benign nevi, atypical nevi and melanomas

	Clearly benign lesions (288)		Atypical nevi (76)		Melanomas (95)	
	Mean	SD	Mean	SD	Mean	SD
PXMED1	28.04	9.40	32.09*	11.46	41.62*,†	18.07
PXVAR1	358.21	292.27	495.37*	376.99	958.55*,†	908.42
PXMAX1	62.33	26.19	77.65*	34.13	113.06*,†	47.75
PXMED2	39.95	9.12	43.05*	10.37	50.11*,†	17.20
PXVAR2	724.08	384.49	889.90*	457.13	1391.43*,†	1037.75
PXMAX2	107.64	24.35	120.80*	32.83	156.68*,†	45.90

SD, standard deviation; PXMED1, mean colour difference; PXVAR1, mean variance of colour difference; PXMAX1, maximum colour difference referring to 1% reduced images; PXMED2, mean colour difference; PXVAR2, mean variance of colour difference; PXMAX2, maximum colour difference referring to 2% reduced images.

*Significant with respect to clearly benign nevi.

†significant with respect to atypical nevi.

diagnostic accuracy (86.6%), a sensitivity of 87.5% and a specificity of 85.7% were obtained. Mean and standard deviation of D values were 2.235 ± 1.665 for MMs and -0.363 ± 0.872 for nevi.

Discussion

The pigment distribution assessment method described in this study subdivides the image into homogeneous blocks, and translates structural differences into RGB colour ones. Details such as globules, dots, regression structures, areas of increased vascularization, or grey–blue areas contribute to RGB values within the image block they are included in. The distribution of these structures is then assessed by comparing RGB values pertaining to different pixels blocks. A big difference between RGB values means that the lesion's structure is non homogeneous and its architecture is complex. This corresponds to structural asymmetry as assessed by the clinician when employing semi-quantitative methods.

In fact, significant differences between parameter values were observed for different ML populations. In MMs, mean and maximum differences between RGB values referring to different image blocks were significantly higher than in nevi, indicating colour variegation and a complex architecture. Moreover, AN were characterized by intermediate values between those referring to MMs and those belonging to nevi.

Pattern analysis represents the basis for the dermoscopic diagnosis of MM (5, 21), however, in early MM, diagnostic structures may be lacking (26, 27). In an early stage, MMs tend to spread laterally and to become asymmetric. Therefore, especially for discriminating *in situ* MMs, great attention has to be paid to network and pigment distribution.

According to Stolz et al. (4), asymmetry assessment of microscopic features (including asymmetric distribution of differential structures and colours) contributes by one-two thirds to MM diagnosis, whereas in the semiquantitative method by Blum et al. (24), structural asymmetry contributes by 25% to the overall score.

In AN, pigment distribution enables a classification for the distinction between different risk levels: according to Hoffmann-Wellenhof et al. (28), the presence of peripheral hyper-pigmentation requires a differential diagnosis with an *in situ* MM.

In a follow-up study performed by Kittler et al. (26), 75-recorded lesions, showing substantial modifications over time, were excised. Among these, eight early MMs were diagnosed, but only four showed structural dermoscopic modifications (26). Moreover, architectural modifications were observed in early MMs arising on moderately atypical or mildly atypical lesions with a history of change, which were monitored during an average period of 3 months by Menzies et al. (27), whereas none of these MMs developed any classic surface microscopic feature of MM.

In order to overcome subjectivity and variability in the interpretation of dermoscopic images, several image analysis programs have been recently introduced as a possible support for clinical diagnosis (6–18). These programs are based on assessment of lesion size, shape, colour, and texture, which are expressed by mathematical parameters.

For the assessment of asymmetry of the lesion Andreassi et al. (13) employed both circularity (defined as the percentage of the lesion not overlapping a circle of equal area), and imbalance of dark areas. A few years ago we measured the distance of dark areas within the lesion from the barycentre, and showed that this parameter has discriminant power (10, 12).

According to Oka et al. (29), who performed image analysis on 59 MM and 188 equivocal Clark nevi, morphological variables (asymmetry and circularity) had a greater weight than the variables used for colors and texture in discriminating between *in situ* MMs and Clark nevi, whereas mean RGB values provided a large contribution to the discrimination of thin invasive MMs from Clark nevi.

As regards pigment distribution, we recently described two different programs for its description in dermoscopic ML images, based on the evaluation of the distribution of dark areas (17). The first method permits the identification of 'absolute' dark areas, defined as areas, which are darker than the skin by an absolute amount. The second identifies the area in the image, which is the darkest with respect to the overall brightness of the lesion ('relative' dark area). A set of parameters for their description was developed and tested on 339 images of melanocytic lesions (ML) acquired by means of a polarized-light videomicroscope. Although in these methods only grey levels were considered and no attention was paid to colours, significant differences in dark area distribution between MMs and nevi

were observed, permitting a good discrimination of ML (diagnostic accuracy = 74.6% and 71.2% for absolute and relative dark areas, respectively).

In this study we are presenting a new method for the assessment of variations in the distribution of pigmentation, which overcomes the concept of asymmetry axis. Each colour block is compared with the others forming the image and not only to its symmetric one. Moreover, measures of colour distribution are obtained for different detail levels depending on the degree of resizing of the image.

In conclusion, since architectural modifications represent the most precocious sign of malignant change, automated assessment of pigment distribution, to be implemented in programs for computer-aided diagnosis of MM, could prove particularly useful for the identification of lesions which should undergo follow-up examinations, as a complement to digital monitoring and dermoscopic observation.

Acknowledgements

This study was partially supported by MIUR (Ministero dell'Istruzione dell'Università e della Ricerca), grant number 2001068929.

References

1. Pehamberger H, Steiner A, Wolff K. In vivo epiluminescence microscopy of pigmented skin lesions. I. Pattern analysis of pigmented skin lesions. J Am Acad Dermatol 1987; 17: 571–583.
2. Kenet RO, Kang S, Kenet BJ et al. Clinical diagnosis of pigmented lesions using digital epiluminescence microscopy. Arch Dermatol 1993; 129: 157–174.
3. Bahmer FA, Fritsch P, Kreusch J et al. Terminology in surface microscopy. J Am Acad Dermatol 1990; 23: 1159–1162.
4. Stolz W, Braun-Falco O, Bilek P et al. Color atlas of dermatoscopy. Oxford: Blackwell Science, 1994.
5. Argenziano G, Soyer HP, Chimenti S et al. Dermoscopy of pigmented skin lesions: results of a consensus meeting via the internet. J Am Acad Dermatol 2003; 48: 679–693.
6. Cascinelli N, Ferrario M, Bufalino R et al. Results obtained by using a computerized image analysis system designed as an aid to diagnosis of cutaneous melanoma. Melanoma Res 1992; 2: 163–170.
7. Green AC, Martin NG, Pfitzner J et al. Computer image analysis in the diagnosis of melanoma. J Am Acad Dermatol 1994; 31: 958–964.
8. Hall PN, Claridge E, Morris Smith JD. Computer screening for early detection of melanoma – is there a future? Br J Dermatol 1995; 132: 325–338.
9. Gutkowicz-Krusin D, Elbaum M, Szwaykowski P, Kopf AW. Can early malignant melanoma be differentiated from atypical melanocytic nevus by in vivo techniques? Part II. Automatic machine vision classification. Skin Res Technol 1997; 3: 15–22.
10. Seidenari S, Pellacani G, Pepe P. Digital videomicroscopy improves diagnostic accuracy for melanoma. J Am Acad Dermatol 1998; 39: 175–181.
11. Binder M, Kittler H, Seeber A et al. Epiluminescence microscopy-based classification of pigmented skin lesions using computerized image analysis and an artificial neural network. Melanoma Res 1998; 8: 261–266.
12. Seidenari S, Pellacani G, Giannetti A. Digital videomicroscopy and image analysis with automatic classification for detection of thin melanomas. Melanoma Res 1999; 9: 163–171.
13. Andreassi L, Perotti R, Rubegni P et al. Digital dermoscopy analysis for the differentiation of atypical nevi and early melanoma. Arch Dermatol 1999; 135: 1459–1465.
14. Pellacani G, Martini M, Seidenari S. Digital videomicroscopy with image analysis and automatic classification as an aid for diagnosis of Spitz nevus. Skin Res Technol 1999; 5: 266–272.
15. Seidenari S, Pellacani G, Grana C. Computer description of colours in dermoscopic melanocytic lesion images reproducing clinical assessment. Br J Dermatol 2003; 149: 523–529.
16. Grana C, Pellacani G, Cucchiara R, Seidenari S. A new algorithm for border description of polarized light surface microscopic images of pigmented skin lesions. IEEE Trans Med Imaging 2003; 22: 959–964.
17. Pellacani G, Grana C, Cucchiara R, Seidenari S. Automated extraction and description of dark areas in surface microscopy melanocityc lesion images. Dermatology 2004; 208: 21–26.
18. Pellacani G, Grana C, Seidenari S. Automated description of colours in polarized-light surface microscopy images of melanocytic lesions. Melanoma Res 2004; 14: 125–130.
19. Menzies SW, Ingvar C, McCarthy WH. A sensitivity and specificity analysis of the surface microscopy features of invasive melanoma. Melanoma Res 1996; 6: 55–62.
20. Argenziano G, Fabbrocini G, Carli P et al. Epiluminescence microscopy for the diagnosis of doubtful melanocytic skin lesions. Comparison of the ABCD rule of dermoscopy and a new 7-point checklist based on pattern analysis. Arch Dermatol 1998; 134: 1563–1570.
21. Braun RP, Rabinovitz H, Oliviero M et al. Pattern analysis: a two-step procedure for the dermoscopic diagnosis of melanoma. Clin Dermatol 2002; 20: 236–239.
22. Mac Kie RM, Fleming C, Mc Mahon AD, Jarret P. The use of the dermatoscope to identify early melanoma using the three-colour test. Br J Dermatol 2002; 146: 481–484.
23. Nachbar F, Stolz W, Merkle T et al. The ABCD rule of dermatoscopy. J Am Acad Dermatol 1994; 30: 551–559.
24. Blum A, Rassner G, Garbe C. Modified ABC-point list of dermoscopy: a simplified and highly accurate dermoscopic algorithm for the diagnosis of cutaneous melanocytic lesions. J Am Acad Dermatol 2003; 48: 672–678.
25. Grana C, Pellacani G, Seidenari S, Cucchiara R. Color Calibration for a Dermatological Video Camera System. Proceedings of IAPR International Conference on Pattern Recognition 2004, in press.
26. Kittler H, Pehamberger H, Wolff K, Binder M. Follow-up of melanocytic skin lesions with digital epiluminescence microscopy: patterns of modifications observed in early melanoma, atypical nevi, and common nevi. J Am Acad Dermatol 2000; 43: 467–476.
27. Menzies SW, Gutenev A, Avramidis M et al. Short-term digital surface microscopic monitoring of atypical or

changing melanocytic lesions. Arch Dermatol 2001; 137: 1583–1589.
28. Hofmann-Wellenhof R, Blum A, Wolf I et al. Dermoscopic classification of atypical melanocytic nevi (Clark nevi). Arch Dermatol 2001; 137: 1575–1580.
29. Oka H, Tanaka M, Kobayashi S, Argenziano G, Soyer HP, Nishikawa T. Linear discriminant analysis of dermoscopic parameters for the differentiation of early melanomas fron Clark nevi. Melanoma Res 2004; 14: 131–134.

Address:
Stefania Seidenari
Department of Dermatology
University of Modena and Reggio Emilia
41100 Modena
Italy

Tel: +39-59 4222464
Fax: +39-59 4224271
e-mail: seidenari.stefania@unimore.it